LIMNOLOGY AND OCEANOGRAPHY
Letters

ASLO
Open Access

Limnology and Oceanography Letters 3, 2018, 302–310
© 2018 The Author. Limnology and Oceanography Letters published by Wiley Periodicals, Inc.
on behalf of Association for the Sciences of Limnology and Oceanography
doi: 10.1002/lol2.10083

SPECIAL ISSUE LETTER

Sediment respiration drives circulation and production of CO_2 in ice-covered Alaskan arctic lakes

Sally MacIntyre,[1,2] *Alicia Cortés*[2] *Steven Sadro*[2,3]

[1]Department of Ecology, Evolution and Marine Biology, University of California at Santa Barbara, Santa Barbara, California; [2]Marine Science Institute, University of California at Santa Barbara, Santa Barbara, California; [3]Department of Environmental Science and Policy, University of California, Davis, California

Scientific Significance Statement

Because arctic lakes are ice-covered for 9 months each year, accurate regional carbon budgets require estimates of winter production of CO_2 and a predictive understanding of CH_4 accumulation. Such measurements are rare due to the difficulties of winter sampling. By combining profile data and in situ instrumentation, we show that sediment respiration is the primary source of CO_2 and production can be predicted using readily measured time series of dissolved oxygen. We extend prior understanding of the overturning circulation typical in ice-covered lakes by showing that the contribution from sediment respiration depends on basin morphometry and sediment organic matter. This mechanistic understanding enables improved modeling of the overturning circulation with implications for the onset of anoxia, accumulation of CH_4, and extent of emissions at ice-off.

Abstract

The goals of our study were to (1) quantify production of CO_2 during winter ice-cover in arctic lakes, (2) develop methodologies which would enable prediction of CO_2 production from readily measured variables, and (3) improve understanding of under-ice circulation as it influences the distribution of dissolved gases under the ice. To that end, we combined in situ measurements with profile data. CO_2 production averaged 20 mg C m^{-2} d^{-1} in a 3 m deep lake and ~ 45 mg C m^{-2} d^{-1} in four larger lakes, similar to experimental observations at temperatures below 4°C. CO_2 production was predicted by the initial rate of loss of oxygen near the sediments at ice-on and by the full water column loss of oxygen throughout the winter. The time series data also showed the lake-size and time dependent contribution of sediment respiration to under-ice circulation and the decreased near-bottom flows enabling anoxia and CH_4 accumulation.

*Correspondence: sally@eri.ucsb.edu

Author Contribution Statement: SM developed the research questions. SM and SS developed the study protocols. SM and AC led the analysis of the time series data, all co-authors contributed to data acquisition, data analysis, and writing of the manuscript.

Data Availability Statement: Time series and profiles of temperature and bio-geochemical variables are archived in the Arctic Data Center repository, and available at: https://arcticdata.io/catalog/#view/urn:uuid:6f5533ab-6508-4ac7-82a3-1df88ed4580e.

Additional Supporting Information may be found in the online version of this article.

This is an open access article under the terms of the Creative Commons Attribution License, which permits use, distribution and reproduction in any medium, provided the original work is properly cited.

This article is part of the Special Issue: Carbon cycling in inland waters
Edited by: Emily Stanley and Paul del Giorgio

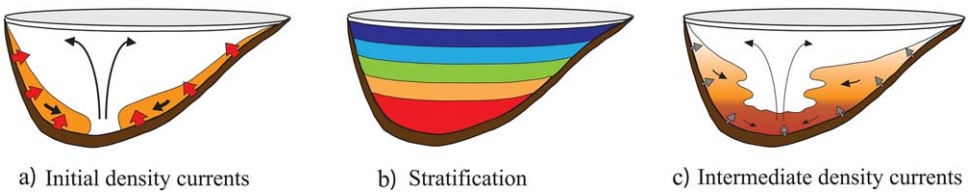

Fig. 1. Hydrodynamic processes and stratification in lakes under the ice. (**a**) Sediment heating of the overlying water at temperatures below 4°C creates density currents which flow downslope; respiration at the sediment–water interface contributes by producing solutes which also increase density (Mortimer and Mackereth 1958). Upward flows balance the downslope flows resulting in an overturning circulation (Welch and Bergmann 1985; Malm 1998; Rizk et al. 2014). (**b**) Heat and solutes become stratified as warm water enriched with the products of respiration flows to the deepest points of lakes. (**c**) As sediment heat fluxes and respiration rates decrease over the winter, later intrusions flow at progressively shallower depths. With reduced flow into the lower layer, anoxia develops and CH_4 may accumulate.

Rates of ecological processes in lakes are often disproportionately high compared to their area thus these ecosystems represent biogeochemical hotspots in the landscape. In particular, processing of carbon by inland waters is now recognized as a significant component of regional and global carbon dynamics (Cole et al. 2007; Raymond et al. 2013; Wik et al. 2016). Despite long periods of ice cover in arctic and sub-arctic lakes and the potential for significant accumulation of CO_2 and CH_4, annual budgets that include the contribution from winter are rare and primarily from shallow lakes (Karlsson et al. 2008, 2013; Jammet et al. 2015; Denfeld et al. 2018). Under-ice transformations of organic matter may be considerable in arctic lakes. Emissions of CO_2 near ice-off can be five times those during the subsequent summer period, and the near-surface supersaturation observed during summer may result, in part, from partial retention of the gases produced during winter (Kling et al. 1991, 1992; S. MacIntyre unpubl.). In addition to the need for quantifying winter respiration and accumulation of CO_2 and CH_4, extrapolating to other lakes across the landscape requires: (1) relating emissions to organic substrates (Wik et al. 2016; Gudasz et al. 2017), (2) approaches to compute CO_2 production when access during winter is difficult, and (3) extending prior understanding of how respiration and sediment heat fluxes structure the water column under the ice to moderate accumulation and emissions of CO_2 and CH_4.

Mortimer and Mackereth's (1958) pioneering under-ice study that linked hydrodynamics and biogeochemistry provides a framework for developing a mechanistic understanding of controls on winter production and distribution of CO_2. Heat fluxes from the sediments and solutes, such as dissolved inorganic carbon, produced by sediment respiration increase the density of the water at the sediment–water interface. This water flows down slope as a density current with slow upward flows expected to balance the downward ones such that an overturning circulation develops (Fig. 1). While depletion of dissolved oxygen at deep locations due to the downslope movement has been described (Terzhevik et al. 2009), links with accumulation and vertical distribution of CO_2 and CH_4 and with potential for evasion at ice-off have not been made.

We used autonomous instruments deployed throughout the winter in five arctic lakes and profile data obtained before ice-on, within a month of ice-on, and under the ice in spring to quantify respiration, CO_2 production, and determine under-ice circulation and extent of anoxia. We tested the hypothesis that winter CO_2 production can be estimated from the rate of drawdown of dissolved oxygen near the sediment–water interface during the initial period of ice formation and from our results infer that CO_2 is produced primarily from sediment respiration. We illustrate under-ice thermal and density structure as well as the time scales for upward flows in a 150 ha and a 1.6 ha lake. Via detailed analysis, we show that the increase in near-bottom density which drives the under-ice overturning circulation is initially from heat flux in the larger lake and solute flux from respiration in the smaller lake. The rapid near bottom increase in density in the smaller lake created conditions favorable for the onset of anoxia and CH_4 accumulation.

Methods

Study sites

Five oligotrophic and net heterotrophic kettle lakes in the northern foothills of the Brooks Range, Alaska, were instrumented and sampled between September 2012 and July 2016 (Table 1). Attributes of lakes in the region including surface area, depths, landscape age, water chemistry, and light attenuation are described in Luecke et al. (2014). The surface area of the basins we studied ranges from 1 ha to 150 ha and their depths from 3 m to 24 m; the depth of the upper mixed layer and thickness of the thermocline during the ice free period are larger for Toolik Lake with its greater wind exposure than for smaller lakes (Luecke et al. 2014). Ice-on and ice-off dates vary with lake size and by year, but typically the lakes are ice-covered by early October and become ice free in June. Snowmelt typically begins in early May, a month prior to ice-off. Ice thickness is spatially variable in each lake and for all lakes the maximum tended to be between 1.0 m and 1.4 m.

Table 1. Characteristics of the lakes, their sub-basins, and watersheds: WA is watershed area; Area is lake or sub-basin surface area. Z_{max} and Z_{mean} are maximum or mean lake and sub-basin depths, respectively; OC shallow and OC deep describe the organic carbon content by weight percent of lake sediments corresponding to shallow and deep sediment core sites; S-Resp are respiration rates measured on sediment cores collected from shallow and deep sites in the autumn; O_2 change-lake is the rate of drawdown of O_2 measured immediately following ice on using data from the deepest logger in each lake or sub-basin. Analysis was conducted in two of Toolik Lake's sub-basins, Toolik Main (TM) and Toolik Inlet Bay (TIB), and in the larger of Lake E1's basins (East).

	Latitude (°)	Longitude (°)	WA (ha)	Area (ha)	Z_{max} (m)	Z_{mean} (m)	k_d^* (m^{-1})	DOC* (mg L^{-1})	OC shallow (%)	OC Deep (%)	S-Resp shallow (mg O_2 m^2 d^{-1})	S-Resp deep (mg O_2 m^2 d^{-1})	O_2 change Lake† (mg O_2 m^2 d^{-1})
Toolik	68.633	−149.607	6688	149.0	26.0	7.4	0.6	6	5–9‡	5–9‡	–	–	–
TM	–	–	–	94.0	24.0	7.0	0.6	6	6 − 9	5.5	298	502	335 (50,3)
TIB	–	–	–	10.7	12.0	4.1	0.6	6	9	–	485	396	333 (27,3)
N2§	68.640	−149.626	22	1.6	10.4	5.0	0.8	6.5	13,17‖	–	432	758	222 (24,3)
E1	68.626	−149.555	89	2.9	12.0	3.1	0.8	6.6	10	–	689	–	–
E1-East	–	–	–	1.8	12.0	3.7	0.8	6.6	–	–	–	727	217 (37,4)
E5§	68.642	−149.458	130	10.9	12.9	6.4	1.1	7	5.5–9	–	444	490	238 (67,3)
E6§	68.643	−149.441	27	1.9	3.0	1.6	1.4	9	24	16	643	643	243 (69,2)

* From Luecke et al. (2014) and ARC LTER database. Landscapes were glaciated over 250,000 yr ago (E5 and E6), 60,000 yr ago (E1), 12,000 yr ago (N2), and 12,000 yr and 60,000 yr ago (Toolik). Bathymetry and watershed area from Jason Stuckey and Randy Fulweber with bathymetry of smaller lakes done in 2013 and Toolik Lake in 2008. Watershed area for Toolik Lake from Kling et al. (2000).

† Standard deviation and number of years in which the measurement was made are in parentheses.

‡ Cornwell and Kipphut (1992). Other data personal communication, Anne Giblin.

§ Lake was experimentally fertilized: N2 (1985–1991), E5 and E6 (2001–2013).

‖ Cores were from 5 m sites. Lower value is from control site, higher is mean from fertilized side of the lake.

Instrumentation and sampling

Meteorological data and high sensitivity biogeochemical arrays used below and through the ice in Toolik Lake are described in Cortés et al. (2017). One array in all lakes was at the deepest part with one or more additional arrays near the margin. Each array included instruments to measure temperature (RBR 1050, 1060, and SoloT: ± 0.002°C), specific conductance (SC) (Onset U24: ± 5 μS cm^{-1}), and dissolved oxygen (DO) (PME MiniDOT: ± 0.3 mg L^{-1}) deployed at 4–7 depths, including a DO sensor within a meter of the bottom (MacIntyre and Cortés 2017). Profile data were obtained using a Hydrolab DS5, JFE Advantech conductivity, temperature, depth (CTD) profiler, and Yellow Springs Instruments Castaway CTD with the latter used monthly over the winter (Cortés et al. 2017). Water samples for CO_2 and CH_4 were collected in all lakes in mid-September prior to ice-on, in November about one month after ice-on, and in late April or early May prior to snowmelt. CO_2 and CH_4 concentrations were measured with the headspace method and gas chromatography (Kling et al. 1991). Gas samples from 2012 to 2013 were injected into glass vials after displacing a saline solution; those in subsequent years were injected into evacuated exetainers. Sediment respiration rates were measured on cores taken from the deepest locations in the lakes and sites along the lake margins in fall. Sediment incubations were conducted in the laboratory under ambient lake temperatures following Daniels et al. (2015).

Computations

Density was computed based on temperature and salinity, with salinity computed from measurements of major ions for all the lakes and regressed against specific conductance (Cortés et al. 2017). Data from fixed instrument moorings were supplemented with profile data to improve accuracy and create a more detailed grid of SC for density calculations. Isotherms and isopycnals, lines of constant density, were computed from linear interpolation of time series temperatures and densities. Upward velocities were computed from the rate of rise of isopycnals. We created a grid of vertical points throughout the water column, calculated the distance of each grid point from the upper density discontinuity caused by the presence of ice or appreciably colder water, and computed the time scales of rise by dividing each distance by velocity (Fig. 2). We computed the CO_2 produced over the winter from the sum of the moles in volume strata computed from the mid-point between measurements, less the moles present just prior to ice-on in September and divided by lake volume when we sampled in late April/early May. CO_2 production was also estimated from the initial rate of drawdown in dissolved oxygen obtained from the oxygen sensors closest to the sediments (Supporting Information Fig. S1). We multiplied this rate by the sensor height, the area of sediments below 3 m, and the time from ice-on until our first sampling in spring. We selected 3 m as rocky substrata decrease below 3 m. Full lake oxygen loss was computed in Toolik Main, Lake N2, and in Lake E1, in years when we had at least five DO sondes in the smaller lakes and six in Toolik Lake, based on the mass present at ice-on and that present on our first sampling date in spring. The latter was calculated from the product of concentration and volume in the depth intervals between DO sensors. To convert these oxygen-based calculations to CO_2, we assumed a respiratory quotient of 1. Production was normalized to mean concentration by dividing the moles produced by lake volume in late April/early May prior to snowmelt. Production on an areal basis was obtained by dividing the mass produced by lake surface area during ice-free conditions.

Results

Immediately after ice-on, near bottom temperatures increased (Fig. 2). This increase provides evidence for downward flowing gravity currents induced by the sediments heating overlying water (Fig. 1). Specific conductivity increased (not shown) and oxygen concentrations decreased (Supporting Information Fig. S1) indicating the further modification of near-bottom waters by respiration. The rising isotherms throughout the winter in Toolik Lake support the inference of upward flow which balanced the downward flows (Figs. 1, 2a). In Lake N2 the water column warmed for a short period and then cooled. Isopycnals rose from the lower to the upper water column in both lakes until arrested by increasing ice thickness and intensified temperature gradients below the ice (Fig. 2b,d). In Toolik Lake their rate of upward rise at times was more rapid than that of the isotherms, and in Lake N2, their upward rise occurred despite falling isotherms. These differences occurred because solutes, when present, make an appreciable contribution to density at temperatures near 4°C in freshwater (Supporting Information Fig. S2), and continuing sediment respiration produced solutes which contributed to flows (Fig. 1).

Rising isopycnals are indicative of the upward flows that are a component of the overturning circulation (Figs. 1, 2). Initially, the upward flow was primarily driven by the increased temperatures from sediment heat flux in Toolik Lake and by the increased SC from respiration in Lake N2 (Fig. 3, Supporting Information Fig. S2). In both lakes, the later rise in isopycnals resulted from the solutes produced by respiration. Observations were similar in Lake E1 where we also had sufficient SC sensors for the analysis (data not shown). Thus, ongoing respiration modified the density structure independently of heat fluxes from the sediments. Sediment respiration drove the overturning circulation in the two smaller lakes whose sediments, based on the sediment respiration rates from cores, were more organic rich than those in Toolik Lake (Table 1).

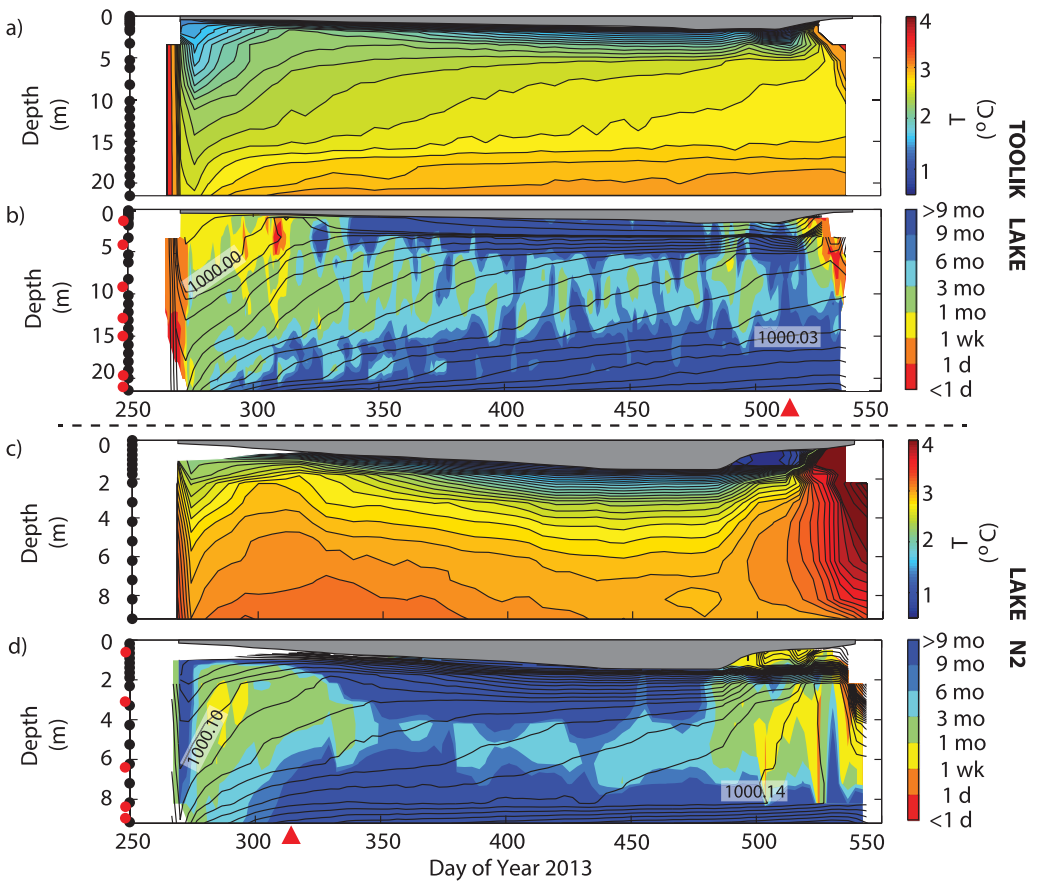

Fig. 2. (**a**, **c**) Inverse thermal stratification and (**b**, **d**) density stratification as isopycnals (lines) and time scales of upward fluxes (colors for days, weeks, and months) in Toolik Lake and neighboring Lake N2 from fall 2013 to spring 2014. Black dots on the *y*-axis (**a**, **c**) indicate the depth of temperature loggers and red dots (**b**, **d**) the depth of SC loggers and typically paired DO sensors. Red arrows mark the onset of anoxia. Gray shapes above the time series data indicate ice thickness and duration. Isotherms and isopycnals were interpolated over 4-d intervals. Isopycnals every 0.0025 kg m^{-3} and 0.005 kg m^{-3} in Toolik Lake and Lake N2, respectively. Density above 1000 kg m^{-3} results from the additional component from solutes. Isotherms are computed at 0.1°C and 1°C intervals below and above 3.5°C, respectively.

Near the sediment–water interface, the rate of upward movement of isopycnals decreased after ice-on as the near-bottom density gradient increased, and the time scale of upward movement near the bottom increased to over 9 months (Fig. 2b,d). Anoxia developed within a month in Lake N2 (Figs. 2d, 3g). Mid-water column in both lakes, the rising time tapered from weeks to 6 months (Fig. 2b,d). The depth dependent changes in rise time indicate reduced ventilation of the lower water column and a larger volume of water intruding above the stronger near-bottom stratification (Fig. 1c). The rise times remained higher for a longer period in winter in Toolik Lake than in Lake N2. The between-lake difference results, in part, from continued introduction of heat and solutes mid-water column in Toolik Lake as opposed to only solutes in Lake N2 (Supporting Information Fig. S2). Continued sediment heat fluxes and persistent downslope flow provide an explanation for the delayed onset of anoxia in Toolik Lake in 2013–2014. However, anoxia was observed to occur over a month earlier in the following winter. The step-like shapes of the DO and CO_2 profiles by late April 2014 provide support for temporally varying intrusion depths (Fig. 3). The level isopycnals in Lake N2 imply lack of exchange with the water above. The continued near bottom rise of isopycnals in Toolik Lake indicates continued upward flow in the full lake.

During spring, additional hydrodynamic processes became operative and modified the rising times. These include penetrative convection (~ day 490), snowmelt (~ day 500), and subsequent penetrative convection (~ day 525). Mixing was not complete by ice-off and solar heating intensified stratification immediately thereafter. The incomplete mixing implies that not all the gases produced over the winter would ventilate, with mixing near the bottom impeded by the increased solute stratification from respiration.

The increased near-bottom SC and the decreased DO are accompanied by increased CO_2 (Fig. 3). For all the lakes, CO_2 produced over the winter was similar to or somewhat less than predictions based on the initial rate of DO

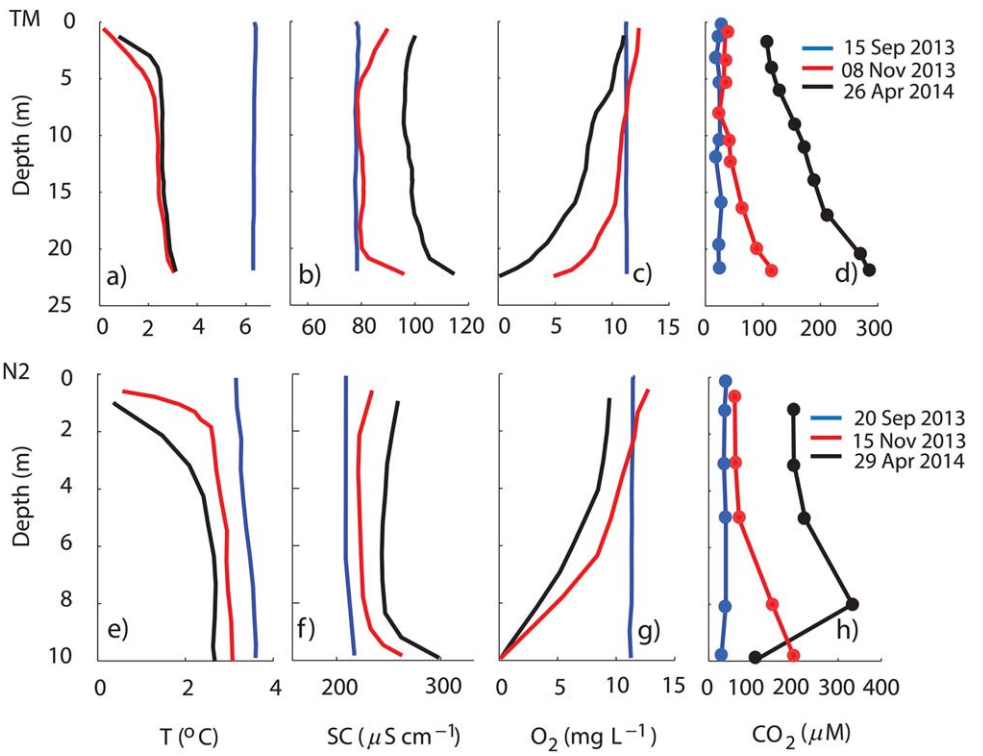

Fig. 3. Profiles in Toolik Lake (TM, upper panels) and Lake N2 (lower panels) of (**a**, **e**) temperature (T), (**b**, **f**) specific conductance (SC); (c, g) dissolved oxygen (O_2); (**d**, **h**) concentration of CO_2 in September 2013 prior to ice-on, in November 2013 approximately one month after ice-on, and in late April 2014 prior to snowmelt. CH_4 did not accumulate in Toolik Lake over the winter. In Lake N2, the concentration of CH_4 in late April was 0.05 μM from the surface to 8 m whereas it increased to 164 μM in the anoxic water at 10 m. We measured T, SC, and O_2 at meter intervals with a Hydrolab DS5. The increases in SC and CO_2 and decreases in O_2 are indicative of respiration, and the resulting CO_2 production is predicted from the initial rate of decrease in oxygen measured above the bottom and the full water column decrease in O_2 using the time series data (Rate, Loss, respectively in Fig. 4).

drawdown at the sediment water interface (Fig. 4). These results imply that the CO_2 primarily was produced by sediment respiration as opposed to respiration in the water column. Loss of oxygen could occur by oxidative processes, such as nitrification (Powers et al. 2017), and confound our interpretation. However, concentrations of both NH_4 and NO_3 are near the limits of detection or at most a few μM in Toolik Lake and nearby lakes indicating that appreciable nitrification over the winter is unlikely to increase the loss of oxygen (MacIntyre et al. 2006; Luecke et al. 2014; ARC LTER database). Rather than the CO_2 that flowed downslope remaining near the sediment water interface, however, the increases higher in the water column in all the lakes resulted from the upward fluxes which balanced the downward flowing gravity currents and from mid-water column intrusions (Fig. 3d,h). The similarity in our calculation of CO_2 produced based on the full water column decrease in oxygen (Fig. 4, loss bars, Supporting Information Fig. S1) relative to that measured and that computed from the initial loss of DO at the sediment water interface (Fig. 4, rate bars), provides further evidence for the upward movement of solutes produced by respiration as opposed to local respiration. We infer that the CO_2 maxima above the bottom in Lake N2 was induced by intrusions above the sharp near-bottom discontinuity (Fig. 3f,h) with similar observations in the other small lakes. Near the bottom, where anoxia was present, CH_4 accumulated (Fig. 3).

Accumulation of CO_2 over the winter was similar in each lake over the 4 yr (Fig. 4). As measured accumulation was similar to or less than that calculated from the initial rate of DO drawdown, we infer that the CO_2 is largely produced by respiration in the sediments and that the computation based on drawdown of DO provides an assessment integrated for the full lake. The inverse relation between mean CO_2 concentration and mean depth of the lakes results, in part, from the larger volume of water in the deeper lakes. Sediment respiration rates, based on sediment cores, tended to be higher from deeper sites than sites along the lake margins (Table 1). Results from Toolik Inlet Basin likely differ from this pattern due to their proximity to Toolik Inlet. With the exception of the main basin in Toolik Lake, where the margin site was at 10 m rather than $\sim$ 2 m as in the other basins, rates at margin sites were 1.4–3 times higher than rates computed based on the initial drawdown in DO (Table 1). As the values of CO_2 production from the rate measurements are similar or higher than measured values (Fig. 4), these comparisons

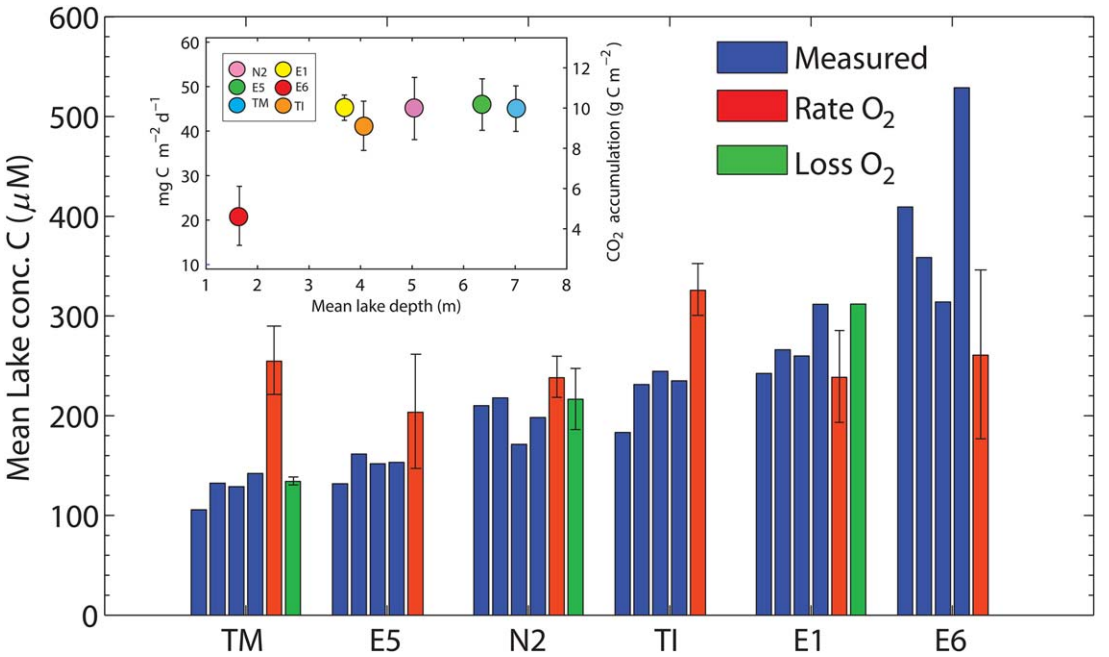

Fig. 4. Volume weighted mean concentrations of CO_2 produced in four winters (2012–2013, 2013–2014, 2014–2015, 2015–2016) for the six basins studied (blue, Measured), and values predicted from rate of oxygen loss near the sediment–water interface immediately after ice-on (red, Rate O_2) and from overall oxygen loss from ice-on until the first day of sampling (green, Loss O_2) (only 1 yr of data was available for this calculation in L. E1). Data are arranged according to mean depth (Table 1). Inset: Daily averaged CO_2 production rates (left axis, mg C m^{-2} d^{-1}) and CO_2 accumulation over 220 ice covered days (g C m^{-2}), where 220 d is approximate time from ice-on until the first sampling date, vs. mean lake depth. Standard deviations are indicated by vertical bars.

imply that whole lake estimates of CO_2 production from sediment cores are too high, likely because of high spatial variability in respiration rates. The initial rate of SC increase was ~ 6 times lower at Toolik Main and in Lake E5 with their lower sediment respiration rates in incubations than in the other lakes (Table 1). Thus, measurements from sediment cores are indicative of respiration potential.

Discussion

Our measurements of CO_2 production and changing hydrodynamics under the ice in five Alaskan arctic lakes indicate that sediment respiration is the primary source of CO_2, provide a basis for extrapolating to other arctic lakes, and illustrate approaches using high resolution time series data for quantifying production in lakes where access is difficult during the ice-covered period. On an areal basis, accumulation of CO_2 was least for the shallow lake, 4 g C m^{-2}, and ranged from 8 g C m^{-2} to 10 g C m^{-2} for the deeper basins (Fig. 4, inset). These values are in the range of those obtained from temperate and boreal lakes (Ducharme-Riel et al. 2015) and a shallow arctic lake (Ramlal et al. 1994). With these limited observations, it is not clear whether production of CO_2 on an areal basis scales with mean depth as observed by Ducharme-Riel et al. (2015). The lower areal production in shallow lakes or lakes with shallow mean depth may be biased low when weighted by lake surface area in the ice-free period. It may also result from colder temperatures above the sediments and resulting lower respiration rates or a shift to anaerobic respiration once the sediments become anoxic with anoxic area relatively larger due to their small volume.

Daily averaged respiration rates, ~ 45 mg C m^{-2} d^{-1} for the deeper lakes, were near the mean value predicted for respiration for water temperatures between 0°C and 4°C (Fig. 4, inset) (Gudasz et al. 2010). Although rates were half as much for Lake E6, they were similar to predictions for oligotrophic lakes at cold temperatures (Gudasz et al. 2010). Areal production of CO_2 was independent of watershed area and implied loading of organic matter and appeared to be independent of prior fertilization as accumulation in recently fertilized Lake E5 was similar to that in unfertilized Toolik Lake (Table 1; Fig. 4). Data are unavailable to assess the contribution from benthic algae, macrophytes, and attached periphyton. These contribute considerably to primary production in summer (Ramlal et al. 1994; Whalen et al. 2008) and respiration by benthic algae accounted for 55% of total CO_2 production in winter in shallow subarctic lakes (Karlsson et al. 2008). Studies of benthic communities and their contribution to sediment organic matter may be warranted to understand controls on CO_2 production in arctic lakes during winter.

The contribution of winter time production of CO_2 relative to that in summer is unknown in these lakes. Prior

emissions of CO_2 from Toolik Lake during the ice-free period averaged 30 mmol m^{-2} d^{-1} over a 9-yr period, which gives an annual average of 3 mol m^{-2} (Kling et al. 1992). Over a 200-d period under the ice, we found, on average, that 0.8 mol m^{-2} accumulated (Fig. 4, inset, units converted). Interpretation of these differences is confounded as summer emissions include the ice-off period when fluxes were up to seven times higher than the mean. Our areal values from the rate of DO drawdown were 10 mmol m^{-2} d^{-1}. As the ice covered period is three times longer than the ice-free period, and using the above rates, the amount of CO_2 produced over the winter is equivalent to the average emissions reported by Kling et al. (1992). Winter production ranged from 11% to 100% of that in summer in 12 shallow subarctic lakes (Karlsson et al. 2013). The scarcity of data in winter to complete annual budgets highlights the need for more measurements in arctic lakes (Denfeld et al. 2018).

The circulation under the ice is an overturning circulation initiated by descending density currents and balanced by slow upward flows (Figs. 1, 2). In lakes a few ha in size and $\sim$ 10 m deep, solutes produced by respiration drove the overturning circulation. In larger lakes, the initial flow was primarily due to the density increases from sediment heat flux and later sustained by solute fluxes from respiration. We extend these observations to take into account respiration potential as measured by respiration rates in intact sediment cores (Table 1). As discussed previously, high respiration potential is correlated with a rapid flux of solutes from the sediments. Depending on bottom slopes, the increased solute flux increases the likelihood that sediment respiration will drive the overturning circulation. It will also cause a more rapid increase in near bottom density with accompanying onset of anoxia and accumulation of CH_4. Sediment respiration also led to or contributed to the sustained rise of isopycnals above the bottom layer within a month of ice-on, with velocities similar to those computed by Malm (1998) and Rizk et al. (2014). These indicate intrusions, which we expect to be depleted in oxygen and enriched in CO_2, flowed into the overlying less stratified water (Fig. 1c). We do not have evidence for two overturning circulation layers rotating in different directions as predicted for lakes with sloping margins (Phillips 1970; Rahm 1985). The overturning circulation may not be maintained in shallow lakes where the strong temperature-induced density gradient below the ice constrains upward flow.

Combined hydrodynamic and biogeochemical processes cause an overturning circulation in ice-covered lakes. Controls on sediment heat content at the onset of ice-on are not yet known, but this analysis suggests greater retention of heat in the larger of our study sites (Fig. 2, Supporting Information Fig. S2). The extent to which internal wave motions, as proposed by Kirillin et al. (2012), or other hydrodynamic processes operative at ice-on moderate fluxes from the sediments and resultant rates of circulation are also not known. We do know that a microbially mediated process, sediment respiration, contributes to circulation for much of the ice-covered period. Our observations provide a basis for further modeling which takes into account spatial and temporal variability in sediment heat fluxes, factors regulating sediment organic carbon content, temperature dependent respiration rates, and within lake hydrodynamics as they vary with basin morphometry. Such effort will establish controls on CO_2 production and on conditions conducive to anoxia and accumulation of CH_4. Increased near-bottom stratification associated with the latter will moderate the extent of mixing at ice-off and the potential for evasion of CO_2 and CH_4 produced over the winter.

References

Cole, J. J., and others. 2007. Plumbing the global carbon cycle: integrating inland waters into the terrestrial carbon budget. Ecosystems **10**: 171–184. doi:10.1007/s10021-006-9013-8

Cornwell, J.C., and G. W. Kipphut. 1992. Biogeochemistry of manganese- and iron-rich sediments in Toolik Lake, Alaska. Hydrobiologia **240**: 45–59. doi:10.1007/BF00013451

Cortés, A., S. MacIntyre, and S. Sadro. 2017. Flowpath and retention of snowmelt in an ice-covered arctic lake. Limnol. Oceanogr. **62**: 2023–2044. doi:10.1002/lno.10549

Daniels, W. C., G. W. Kling, and A. E. Giblin. 2015. Benthic community metabolism in deep and shallow Arctic lakes during 13 years of whole–lake fertilization. Limnol. Oceanogr. **60**: 1604–1618. doi:10.1002/lno.10120

Denfeld, B. A., H. M. Baulch, P. A. del Giorgio, S. E. Hampton, and J. Karlsson. 2018. A synthesis of carbon dioxide and methane dynamics during the ice-covered period of northern lakes. Limnol. Oceanogr. Lett. **3**. doi: 10.1002/lol2.10079

Ducharme-Riel, V., D. Vachon, P. A. del Giorgio, and Y. T. Prairie. 2015. The relative contribution of winter under-ice and summer hypolimnetic CO_2 accumulation to the annual CO_2 emissions from northern lakes. Ecosystems **2**: 547–559. doi:10.1007/s10021-015-9846-0

Gudasz, C., D. Bastviken, K. Steger, K. Premke, S. Sobek, and L. J. Tranvik. 2010. Temperature-controlled organic carbon mineralization in lake sediments. Nature **466**: 478–481. doi:10.1038/nature09186.

Gudasz, C., M. Ruppenthal, K. Kalbitz, C. Cerli, S. Fiedler, Y. Oelmann, A. Andersson, and J. Karlsson. 2017. Contributions of terrestrial organic carbon to northern lake sediments. Limnol. Oceanogr. Lett. **2**: 218–227. doi:10.1002/lol2.10051.

Jammet, M., P. Crill, S. Dengel, and T. Friborg. 2015. Large methane emissions from a subarctic lake during spring thaw: Mechanisms and landscape significance. J. Geophys. Res. Biogeosci. **120**: 2289–2305. doi:10.1002/2015JG003137

Karlsson, J., J. Ask, and M. Jansson. 2008. Winter respiration of allochthonous and autochthonous organic carbon in a

subarctic clear-water lake. Limnol. Oceanogr. **53**: 948–954. doi:10.4319/lo.2008.53.3.0948

Karlsson, J., R. Giesler, J. Persson, and E. Lundin. 2013. High emission of carbon dioxide and methane during ice thaw in high latitude lakes. Geophys. Res. Lett. **40**: 1123–1127. doi:10.1002/grl.50152

Kirillin, G., and others. 2012. Physics of seasonally ice-covered lakes: A review. Aquat. Sci. **74**: 659–682. doi: 10.1007/s00027-012-0279-y

Kling, G. W., G. W. Kipphut, and M. C. Miller, 1991. Arctic lakes and streams as gas conduits to the atmosphere: Implications for tundra carbon budgets. Science **251**: 298–301. doi: 10.1126/science.251.4991.298

Kling, G. W., G. W. Kipphut, and M. C. Miller. 1992. The flux of CO_2 and CH_4 from lakes and rivers in arctic Alaska. Hydrobiologia **240**: 23–36. doi:10.1007/BF00013449

Kling, G. W., G. W. Kipphut, M. C. Miller, and W. J. O'Brien. 2000. Integration of lakes and streams in a landscape perspective: The importance of material processing on spatial patterns and temporal coherence. Freshw. Biol **43**: 477–497. doi: 10.1046/j.1365-2427.2000.00515.x

Luecke, C., and others. 2014. The response of lakes near the Arctic LTER to environmental change, p. 238–286. In J. Hobbie and G. Kling [eds.], Alaska's changing Arctic: Ecological consequences for tundra, streams and lakes. Oxford Univ. Press.

MacIntyre, S., and A. Cortés. 2017. Temperature and biogeochemical data from Toolik Lake, Lake N2, Lake E1, Lake E5, and Lake E6, North Slope, Alaska. Arctic Data Center. doi:10.18739/A2X54S

MacIntyre, S., J. O. Sickman, S. A. Goldthwait, and G. W. Kling. 2006. Physical pathways of nutrient supply in a small, ultra-oligotrophic lake during summer stratification. Limnol. Oceanogr. **51**: 1107–1124.

Malm, J. 1998. Bottom buoyancy layer in an ice-covered lake. Water Resour. Res. **34**: 2981–2993. doi:0.1029/98WR01904

Mortimer, C. H., and F. J. H. Mackereth. 1958. Convection and its consequences in ice-covered lakes. Verh. Internat. Verein. Limnol. **13**: 923–932. doi:10.1080/03680770.1956.11895490

Phillips., O. M. 1970. On flows induced by diffusion in a stably stratified fluid. Deep-Sea Res. **17**: 435–443. doi: 10.1016/0011-7471(70)90058-6

Powers, S. M., H. M. Baulch, S. E. Hampton, S. G. Labou, N. R. Lottig, and E. H. Stanley. 2017. Nitrification contributes to winter oxygen depletion in seasonally frozen forested lakes. Biogeochemistry **136**: 119–129. doi:10.1007/s10533-017-0382-1

Rahm, L. 1985. The thermally forced circulation in a small, ice-covered lake. Limnol. Oceanogr. **30**: 1122–1128. doi: 10.4319/lo.1985.30.5.1122

Ramlal, P. S., R. H. Hesslein, R. E. Hecky, E. J. Fee, J. W. M. Rudd, and S. J. Guildford. 1994. The organic carbon budget of a shallow Arctic tundra pond on the Tuktoyaktuk Peninsula, N.W.T., Canada. Biogeochemistry **24**: 145–172. doi:10.1007/BF00003270

Raymond, P. A., and others. 2013. Global carbon dioxide emissions from inland waters. Nature **503**: 355–359. doi: 10.1038/nature12760.

Rizk, W., G. Kirillin, and M. Lepparanta. 2014. Basin-scale circulation and heat fluxes in ice-covered lakes. Limnol. Oceanogr. **59**: 445–464. doi:10.4319/lo.2014.59.02.0445

Terzhevik, A., and others. 2009. Some features of the thermal and dissolved oxygen structure in boreal, shallow ice-covered Lake Vendyurskoe, Russia. Aquat. Ecol. **43**: 617–627. doi:10.1007/s10452-009-9288-x

Welch, H. E., and M. A. Bergmann. 1985. Water circulation in small Arctic lakes in winter. Can. J. Fish. Aquat. Sci. **42**: 506–520. doi:10.1139/f85-068

Whalen, S. C., B. A. Chalfant, and E. N. Fischer. 2008. Epipelic and pelagic primary production in Alaskan arctic lakes of varying depth. Hydrobiologia **614**: 243–257. doi: 10.1007/s10750-008-9510-1

Wik, M., R. K. Varner, K. W. Anthony, S. MacIntyre, and D. Bastviken. 2016. Climate-sensitive northern lakes and ponds are critical components of methane release. Nat. Geosci. **9**: 99–106. doi:10.1038/ngeo2578

Acknowledgments

We thank Jade Lawence, Erik Young, Analisa Skeen, Katie Ringler, Adam T. Crowe, John Lenters, John Melack, Caitlin Rushlow, Andres Gomez-Giraldo, and Ricardo Roman Botero for assistance with field work; Jade Lawrence and Erik Young for assistance with water sample processing and analysis; David Valentine for use of his laboratory for measurement of CO_2 and CH_4; Kevin Kahlmark of the Kellogg Biological Laboratory for analysis of CO_2 and CH_4 in 2015–2016; James O. Sickman for measurement of major ions, Andrea Hagedorn for analysis of alkalinity, and Anne Giblin for use of her sediment corer and oxygen probes for measuring sediment respiration. John Melack, Emily Stanley, and two anonymous reviewers critically read the manuscript. We thank the staff of the U.A.F. Toolik Field station for help with all aspects of logistics and Jebediah Timm and Joseph Franich for assistance with winter thermistor chain, snow camera, and CTD deployments. We thank the ARC LTER for sharing meteorological and CTD data and providing access to boats; the UAF IAB Environmental Data Center for meteorological data (Environmental Data Center Team. 2012–2016; Meteorological monitoring program at Toolik, Alaska. Toolik Field Station, Institute of Arctic Biology, University of Alaska Fairbanks, Fairbanks, AK 99775. http://toolik.alaska.edu/edc/abiotic_monitoring/data_query.php) and use of shared equipment; and Jason Stuckey and Randy Fulweber of the UAF IAB Geographical Information Systems unit for bathymetry and watershed areas. Meteorological datasets provided by the Toolik Field Station Environmental Data Center are based upon work supported by the National Science Foundation under grants 455541 and 1048361. The ARC LTER was funded by NSF DEB-1026843. This project was supported by the U.S. National Science Foundation Grants ARC 1204267 and 1737411 to SM.

Submitted 23 June 2017
Revised 26 March 2018; 01 February 2018
Accepted 29 March 2018